Evidence of structurally continuous collagen fibrils in tendon

Svensson, Rene B; Herchenhan, Andreas; Starborg, Tobias; Larsen, Michael; Kadler, Karl E; Qvortrup, Klaus; Magnusson, Stig Peter

Published in:
Acta Biomaterialia

DOI:
10.1016/j.actbio.2017.01.006

Publication date:
2017

Document version
Publisher's PDF, also known as Version of record

Acta Biomaterialia 50 (2017) 293–301

Contents lists available at ScienceDirect

Acta Biomaterialia

journal homepage: www.elsevier.com/locate/actabiomat

Full length article

Evidence of structurally continuous collagen fibrils in tendons

Rene B. Svensson [a,*], Andreas Herchenhan [a], Tobias Starborg [b], Michael Larsen [c], Karl E. Kadler [b], Klaus Qvortrup [c], S. Peter Magnusson [a]

[a] Institute of Sports Medicine Copenhagen, Department of Orthopedic Surgery M, Bispebjerg Hospital and Center for Healthy Aging, Faculty of Health and Medical Sciences, University of Copenhagen, Copenhagen, Denmark
[b] Wellcome Trust Centre for Cell-Matrix Research, Faculty of Biology, Medicine and Health, University of Manchester, Manchester M13 9PT, United Kingdom
[c] Core Facility for Integrated Microscopy, Department of Biomedical Sciences, Faculty of Health and Medical Sciences, University of Copenhagen, Copenhagen, Denmark

ARTICLE INFO

Article history:
Received 5 October 2016
Received in revised form 5 December 2016
Accepted 3 January 2017
Available online 5 January 2017

Keywords:
Collagen fibril length
FIB-SEM
Focused ion beam
Serial block face-scanning electron microscopy
tendo m. stapedius

ABSTRACT

Tendons transmit muscle-generated force through an extracellular matrix of aligned collagen fibrils. The force applied by the muscle at one end of a microscopic fibril has to be transmitted through the macroscopic length of the tendon by mechanisms that are poorly understood. A key element in this structure-function relationship is the collagen fibril length. During embryogenesis short fibrils are produced but they grow rapidly with maturation. There is some controversy regarding fibril length in adult tendon, with mechanical data generally supporting discontinuity while structural investigations favor continuity. This study initially set out to trace the full length of individual fibrils in adult human tendons, using serial block face-scanning electron microscopy. But even with this advanced technique the required length could not be covered. Instead a statistical approach was used on a large volume of fibrils in shorter image stacks. Only a single end was observed after tracking 67.5 mm of combined fibril lengths, in support of fibril continuity. To shed more light on this observation, the full length of a short tendon (mouse stapedius, 125 μm) was investigated and continuity of individual fibrils was confirmed. In light of these results, possible mechanisms that could reconcile the opposing findings on fibril continuity are discussed.

Statement of Significance

Connective tissues hold all parts of the body together and are mostly constructed from thin threads of the protein collagen (called fibrils). Connective tissues provide mechanical strength and one of the most demanding tissues in this regard are tendons, which transmit the forces generated by muscles. The length of the collagen fibrils is essential to the mechanical strength and to the type of damage the tissue may experience (slippage of short fibrils or breakage of longer ones). This in turn is important for understanding the repair processes after such damage occurs. Currently the issue of fibril length is contentious, but this study provides evidence that the fibrils are extremely long and likely continuous.

1. Introduction

Connective tissues play a crucial role in maintaining the structure of our bodies. The feat of literally keeping us in shape is made no less impressive by the fact that it is performed to a large extent by a single group of proteins called collagens. While there are 28 different types of collagen in vertebrates, it is a subgroup of fibrillar collagens (type I, II, III, V, XI), which is mainly responsible for providing mechanical strength on larger scales [1,2]. The different fibrillar collagens have similarities in their structure and general behavior, and although important differences exist, they all form elongated triple-helical molecules that aggregate in a highly ordered stagger to form fine threads called fibrils [3,4]. These fibrils are the main building blocks of large connective tissues such as skin, bone, cartilage, and tendon. Tendons are possibly some of the simplest connective tissues in terms of structure and composition, consisting almost entirely of parallel type I collagen fibrils [2], with a low rate of turnover [5,6]. In spite of this apparent simplicity, a fundamental question remains unanswered; how long are the fibrils? The diameters of tendon collagen fibrils are routinely measured by transmission electron microscopy (40–400 nm) [7]; however, determining the length has proven more difficult primarily

* Corresponding author at: Institute of Sports Medicine Copenhagen, Bispebjerg Hospital, 8.1, Bispebjerg Bakke 23, 2400 Copenhagen NV, Denmark.
E-mail address: svensson.nano@gmail.com (R.B. Svensson).

http://dx.doi.org/10.1016/j.actbio.2017.01.006
1742-7061/

because individual fibrils are too thin to image by light microscopy methods, they cannot be extracted intact from tissues [8], and they are too long to trace by conventional serial section transmission electron microscopy. Had the length of mature fibrils been on the order of tens or hundreds of microns, it would undoubtedly have been determined many years ago as is the case in embryonic tissue where the lengths are indeed in this range [9].

Tendon is known to have poor healing capabilities, regenerating slowly and often with incomplete recovery [10,11]. Several factors likely play a role in this poor healing ability, including low cell density and vascularization [12] but the tendon structure itself may also play a role due to difficulty in aligning, tensioning, and interweaving new fibrils across a rupture site. For this reason, the length of collagen fibrils is of importance for tendon regeneration, and it is also important in determining how load is distributed through lateral and longitudinal transfer mechanisms.

The question of fibril length in mature tissue has been addressed in the past by several different approaches. Direct structural investigations have attempted to trace the length of fibrils with scanning electron microscopy of fracture surfaces [13] as well as serial sectioning with transmission electron microscopy [14]. Fibril length has also been estimated indirectly based on calculations from mechanical [15] or structural [14] properties. Other studies did not numerically estimate the length but concluded that they are discontinuous by structural and mechanical relations [16,17]. The findings generally agree that mature collagen fibrils are long (>1 mm); however, the direct structural studies find values high enough to indicate that fibrils may be structurally continuous whereas those based on more indirect methods tend to support discontinuity (length < 10 mm).

The aim of the present study was to determine if mature human tendon collagen fibrils are structurally continuous, by tracing individual collagen fibrils over distances in the centimeter range using automated electron microscopy serial imaging techniques. Tracing individual fibrils over such distances turned out not to be possible, instead continuity was investigated in a much shorter (125 μm) mouse tendon (*tendo m. stapedius*) in combination with statistical analyses of mature human tendon fibrils traced over 25 μm segments.

2. Materials and methods

2.1. Human tendons

As part of a previously published study [18], tendon tissue from males 18 to 32 years old were collected during routine anterior cruciate ligament reconstruction, and for the present study a patellar tendon and a hamstring tendon were investigated. The experiment was approved by the ethical committee and informed consent was obtained from the patients as previously described [18]. The patellar tendon was stored frozen at −20 °C in PBS until use while the hamstring tendon was prepared fresh. Frozen storage damages cellular structures but had no observable effect on the collagen. For the patellar tendon, a single fascicle was fixated in glutaraldehyde fixative (2% v/v in 50 mM sodium phosphate buffer, pH 7.2) under low tension (0.2 N) to improve long range alignment. For technical reasons described in the discussion we gave up on using stacks in the mm range obviating the need for long range alignment. Consequently the hamstring tendon was fixated directly in glutaraldehyde without tension.

2.2. Mouse stapedius tendon

Two mature 12-week old mice were pre-anaesthetized with inhalation of Halothane 3% (Halocarbon Laboratories, River Edge, NJ, USA). Anesthesia was induced by intraperitoneal injection with Pentothal Sodium (Abbott Scandinavia AB, Sweden), 55 mg/kg body weight. The mice were fixed by vascular perfusion through the left ventricle of the heart with glutaraldehyde fixative for 5 min. Following fixation, the stapes and the stapedius muscle with the interposed tendon were isolated by microdissection from the middle ear (Fig. 1A). The samples were subsequently transferred to a hypotonic fixative (1% glutaraldehyde in 25 mM cacodylate buffer, pH 7.2) for 1 h to help swell the tendon. Finally, the samples were post-fixed, stained, dehydrated, and embedded as described below.

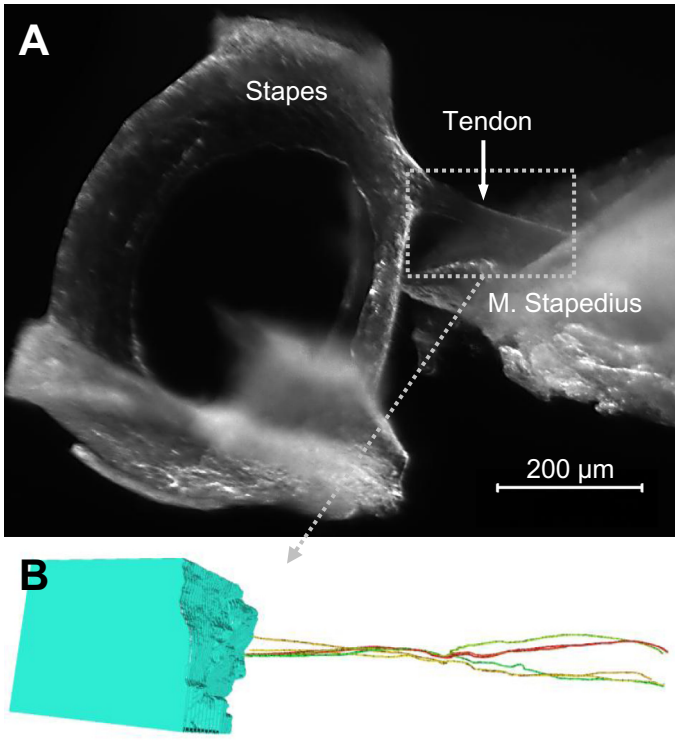

Fig. 1. Mouse stapedius tendon. (A) Stereo microscope image of an isolated stapedius tendon attached to bone (Stapes) and muscle (M. Stapedius). (B) Electron microscope 3D rendering of the 5 collagen fibrils, which were traced through the length of the mouse stapedius tendon. The region to the left is the mineralized fibrocartilage at the bone end. See also Supplementary video 1.

2.3. Sample preparation

Staining and embedding samples for FIB-SEM followed a protocol similar to that of Starborg et al. [19]. Following primary fixation, samples were washed (3 × 20 min) in 0.15 M phosphate buffer (pH 7.2), fixed in 1% OsO_4 with 0.05 M $K_3Fe(CN)_6$ in 0.12 M cacodylate buffer (pH 7.2) (1 h), and subsequently washed in distilled water (3 × 15 min). To enhance the stain, samples were treated with 1% tannic acid in 0.1 M cacodylate buffer (pH 7.2) at 4 °C (1 h), washed in distilled water (3 × 15 min) and stained in 1% OsO_4 in distilled water (1 h) followed by another wash in distilled water (3 × 15 min). Finally, the samples were *en bloc* stained with 1% uranyl acetate in distilled water at 4 °C over night and subsequently washed in distilled water (3 × 15 min). The stained samples were dehydrated in a gradient of ethanol (70% 2 × 15 min, 96% 2 × 15 min, 100% 3 × 15 min), transferred to propylene oxide (2 × 15 min) and subsequently infiltrated with a gradient of epoxy resin (TAAB 812, TAAB Laboratories Equipment Ltd, England) in propylene oxide (25% 40 min, 50% 40 min, 75% 40 min, 100% over night).

Following epoxy infiltration, the human tendon samples were placed in a mold, oriented for transverse sectioning and the resin was cured at 60 °C for 24 h. Resin blocks were trimmed with a razor blade and to reduce "curtaining" artifacts a thin layer of fresh resin was applied to the cut surfaces and polymerized for 24 h. For the mouse stapedius samples, after epoxy infiltration, but before curing the resin, most of the muscle and bone was trimmed away. After partial curing (12 h, 60 °C) the epoxy block was trimmed down to a minimal size parallel to the tendon and completely cured (24 h, 60 °C). Before final imaging, the blocks were sputter coated with 4 nm gold (Leica ACE 200, Vienna, Austria).

2.4. Serial block-face imaging

To visualize the human tendon collagen fibrils in three dimensions a combined focused ion beam and scanning electron microscope (FIB-SEM) was used for acquiring serial block-face images (Quanta FEG 3D, FEI, Eindhoven, Netherlands) [20]. Briefly, after a wide ion beam rough-cut of the exposed sample surface, a field with a well-defined fibril area was selected. Platinum (1 μm) was deposited on the flat surface perpendicular to the mesa in a field that matched the preferred magnification [20]. Trenches were milled on both sides of the platinum deposition [20]. Finally, a fiducial was milled on the platinum layer to aid in alignment.

Image stacks (500–1000 images) were acquired using the software package Slice and View G2 (FEI) by sequentially milling 30 or 50 nm thick slices off the block surface with a gallium ion beam. Between each slice the block surface was scanned by the electron beam and images collected on a retractable backscattered electron detector (vCD, FEI). The electron beam was operated at spot 1, 5.0 kV high tension (HT) at a chamber pressure of 0.3 mPa. The ion beam was operated at 0.5 nA, 30.0 kV HT and working distance 10 mm. Grey scale images were recorded with 8 bit, 2048 × 1768 pixels and 3.0 μs dwell time. The horizontal field width varied between stacks but was typically around 5 μm, with pixel dimensions ~3–5 nm/pixel.

Different equipment was used for the mouse stapedius tendon. A Quanta 250 FEG (FEI) microscope equipped with a 3view ultramicrotome (Gatan, UK) was used to generate serial sections. The SEM was operated at spot 3.5, 4.0 kV, at low vacuum (45 Pa). Images were collected after every 100 nm slice using DigitalMicrograph software (Gatan, UK). Initially a stack was made with 120 μm × 120 μm^2 field of view to contain the entire stapedius tendon, but at this magnification it proved impossible to trace individual fibrils. The stack used in the present study selected a smaller region (6000 × 6000 pixels at 5.2 nm equating to ~30 μm × 30 μm), however, due to the smaller field of view, the tendon insertion into the muscle was initially missed. Consequently the stack starts a few micrometers below the muscle insertion. The field of view had to be manually adjusted an additional 6 times during the recording to keep the tendon in view. The raw data was converted to an MRC stack and the individual regions realigned using IMOD [21] as in Starborg et al. [19].

2.5. Analysis of structural features

All image stacks were analyzed using Amira software (v.5.4, FEI). Individual fibrils were selected on the first frame and traced manually through the image stacks in order to determine fibril ends and other structural features. Initially attempts were made to determine the feasibility of an automated tracing procedure, but the contrast, resolution, and quality of the images did not allow for consistently successful automated segmentation, which is required to trace structures through several hundred images. The advantage of manual tracing is mainly the incorporation of logic, i.e. when multiple small fibrils converge into one indistinguishable bundle over part of the stack, but later split up into the same number of fibrils with the same respective dimensions, it was concluded that they were the same continuous fibrils. It is possible that a more advanced tracking algorithm incorporating such logic could be developed.

Mean fibril length was estimated based on statistics using the number of observed ends and the combined fibril length examined. The formula is essentially the same as previously derived by Starborg et al. [19], but because the present study only traces fibrils from the top frame in the stack, only half the ends will be observed and therefore the length estimate is halved. The basic assumptions are that fibril ends are uniformly distributed in the tissue, that fibrils are longer than the depth of the stack and that their lengths are uniformly distributed around the mean.

$$L_{Fibril} = \frac{L_{Combined}}{n_{Ends}} \quad (1)$$

L_{Fibril} is the estimated mean fibril length in the sample, $L_{Combined}$ is the combined length of all fibril segments traced and n_{Ends} is the observed number of ends amongst the traced segments.

2.6. Fibril dimensions

Changes in fibril diameter along their length were measured in the human tendons by a semi-automated and a manual approach. In the semi-automated method, five equally spaced sections were taken from the image stack (at approximately 0, 6, 12, 18, and 24 μm depth) and each section was analyzed in ImageJ (v.1.46r, National Institute of Health, USA, [22]). Segmentation involved smoothening of the section using de-speckle and Gaussian blur, followed by background subtraction based on a moving cone. Images were subsequently thresholded, and coalesced fibrils were separated with the watershed function. Finally, the particle analysis function was used to determine the cross-sectional area of each fibril. In each of the patella and hamstring tendon 100 fibrils were manually registered to determine corresponding fibrils in each section. Cross-sectional areas were calculated into diameters assuming circularity. A manual method was used to generate a more detailed view of fibril dimensional changes over length. Fibril diameter was measured manually throughout the stack at 500 nm intervals. Fibrils were fairly circular when separate but they appeared elliptical when partially coalesced with neighboring fibrils. Therefore the smallest diameter was measured. The same manual measurement of diameter was also performed on 300 fibrils from a single section on the stapedius tendon for comparison.

3. Results

Throughout the sections, 1021 individual fibrils were traced on the hamstring tendon and 1680 on the patellar tendon, each over approximately 25 μm for a total fibril length of 25.5 mm on the hamstring and 42.0 mm on the patellar tendon (Fig. 2A-B). There were no apparent differences between the two tissues; therefore subsequent analysis considered them as one. In addition to the human tendons, 50 fibrils were traced through the mouse stapedius tendon (tendon length ~125 μm). Most of these fibrils could not be traced throughout the entire length because they either diverged out of the field of view, entered a particularly blurry region of the image, or were disrupted by small cracks, which had likely formed due to stresses in the sample block during microtome sectioning. However, none of the fibrils displayed an actual end, and 5 fibrils were successfully traced through the full length of the tendon (Fig. 1B).

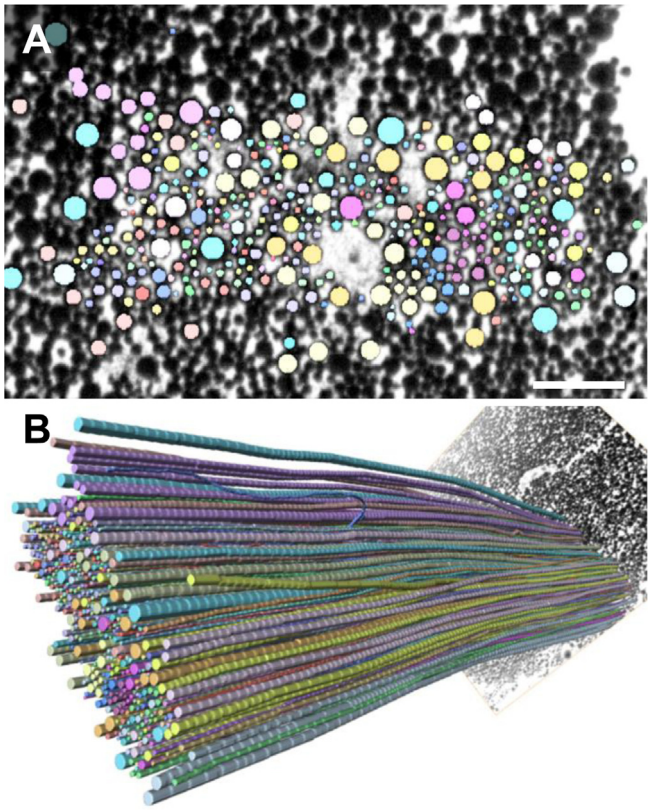

Fig. 2. Illustration of fibril tracing through the tendon. (A) The first section in a FIB-SEM stack with a region of ~300 individual collagen fibrils manually segmented. Scale bar = 1 μm. (B) The same fibrils in a 3D rendering. See also Supplementary videos 2 and 3.

3.1. Structural features

Amongst all the traced fibrils, a single fibril end was observed, which was in the patellar tendon sample. The terminating fibril was thin (45 nm) but did not display noticeable taper. The fibril curved back on itself twice, once right before terminating and once about 20 μm deeper in the specimen (Fig. 3A-D). Seven other fibrils were also observed to curve back on themselves forming a hairpin loop (4 in hamstring and 3 in patellar tendon) (Fig. 4A-C). Three fibrils were observed with grossly irregular structure (1 in hamstring and 2 in patellar tendon) (Fig. 4D-F). Finally, fibril branching points were observed on 4 occasions (all 4 in the same image stack on patellar tendon) (Fig. 5A-D).

Based on the single observed fibril end, the estimated fibril length (Eq. (1)) is equal to the total traced length of 67.5 mm. Due to the low number of observations, the statistical certainty of this number is low. Using binomial statistics, the 95% confidence interval can be estimated by finding the largest fibril length (lowest probability of an end) that would – with 95% probability – have yielded less than one observed end (upper limit) or the shortest fibril length that would – with 95% probability – produce more than one observed end (lower limit). Using this approach, the 95% confidence interval on fibril length becomes 14–1228 mm.

Since the upper confidence limit is much greater than the actual patellar tendon length (~50 mm) an alternative interpretation of the data is to consider two fibril populations, one that spans the length of the tendon and has no ends, and another that is discontinuous with a length up to 50 mm. Using this approach the lower confidence limit could be described by 100% discontinuous fibrils with an average length of 14 mm, the mean value would be equivalent to 26% continuous fibrils and 74% discontinuous fibrils with a length of 50 mm and the upper confidence limit would be consistent with a population of 96% continuous fibrils and 4% discontinuous fibrils with a length of 50 mm. If the assumed length of the discontinuous fibrils was shorter, their proportion would also be reduced.

3.2. Fibril dimensions along their length

Average values for the measured human tendon fibrils are reported in Table 1. To elucidate the dimensional variability of the collagen fibrils the standard deviation and coefficient of variation along each fibril was determined. There was no relation between fibril diameter and the within-fibril standard deviation. We interpret this fairly constant variance as measurement uncertainty resulting from the somewhat blurred fibril outlines (Fig. 3B-D), rather than a functional modulation to fibril diameter. Manual diameter measurements along the fibrils (Fig. 6), providing greater longitudinal resolution (50 measurement sites vs. 5), were in good agreement with the semi-automated method (Table 1). In addition to the diameter variability we also investigated if taper was apparent. The average absolute slope (i.e. independent of taper direction) was 0.56 nm/μm. Assuming that taper is only present

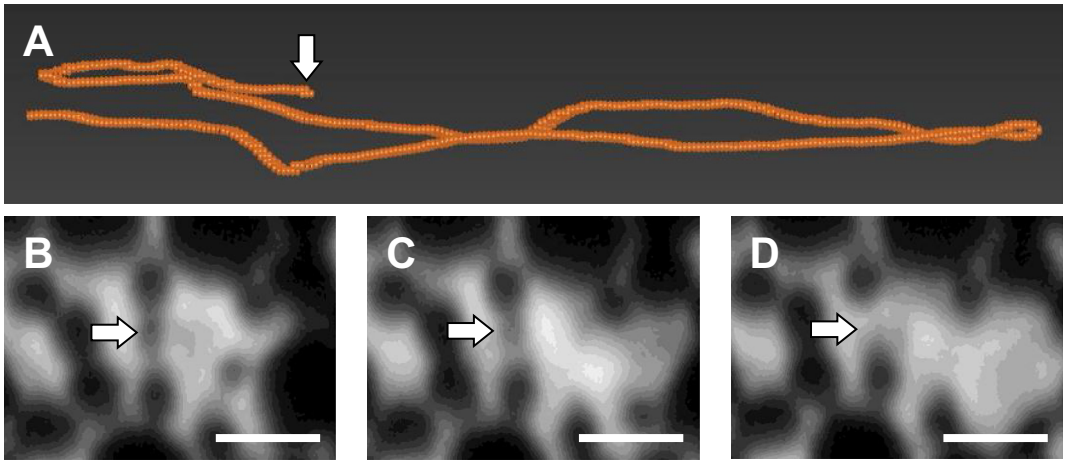

Fig. 3. Illustration of the only observed fibril end. (A) 3D rendering of the whole fibril, the width of the image is 11 μm. It forms a hairpin loop towards both the left and the right. Arrow marks the end. (B-D) Consecutive FIB-SEM sections (~500 nm apart) of the fibril end. Arrows mark the ending fibril. Scale bar = 150 nm. See also Supplementary videos 4 and 5.

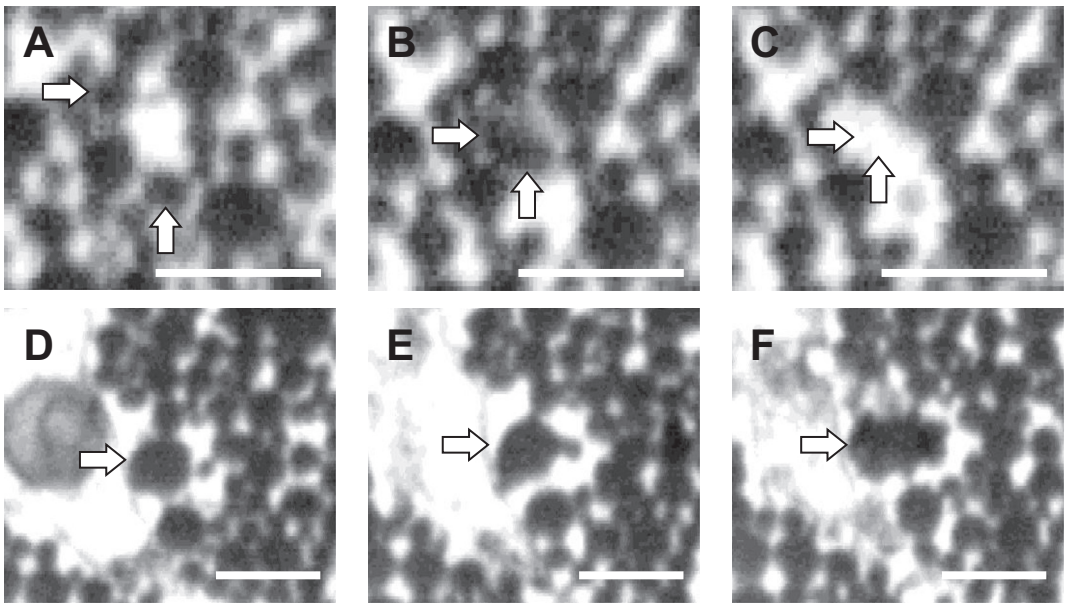

Fig. 4. Observed structural features. (A-C) Consecutive FIB-SEM sections (~500 nm apart) through a looping collagen fibril. The fibril initially appears as two separate fibrils of equal size. The two fibrils then merge and finally both fibrils disappear. Arrows mark the looping fibril. Scale bar = 500 nm. See also Supplementary video 6. (D-F) Consecutive FIB-SEM sections (~500 nm apart), showing a large collagen fibril changing from a circular to an irregular shape. Arrows mark the irregular fibril. Scale bar = 500 nm. See also Supplementary video 7.

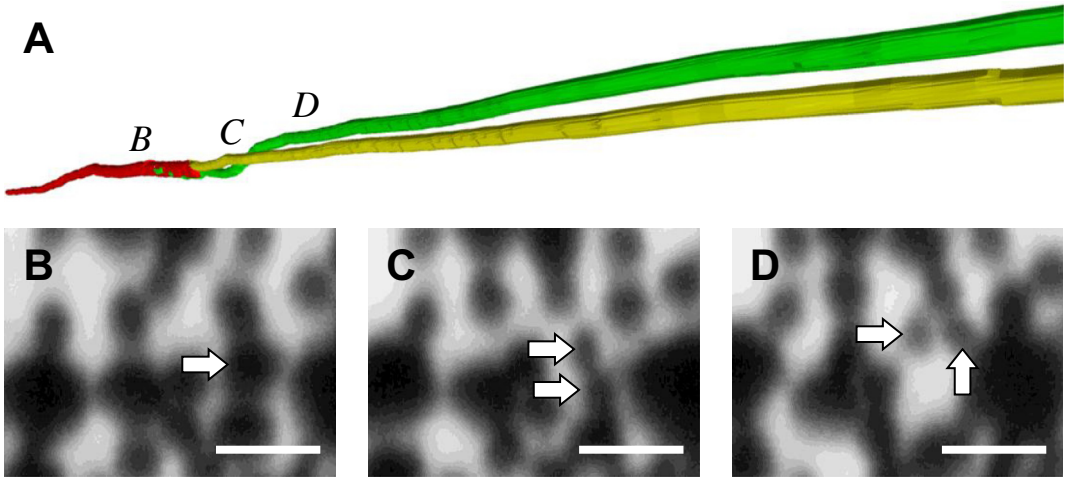

Fig. 5. Illustration of a branching fibril. (A) 3D rendering of a branched fibril. Letters refer to the approximate location of the images in B-D. (B-D) Consecutive FIB-SEM sections (~500 nm apart) of the branching point. Arrows mark the initially merged and subsequently split fibrils. Scale bar = 150 nm. See also Supplementary video 8.

Table 1
Variation in fibril dimensions along their length. Mean (SD) [range].

	Fibril Diameter* (nm)	Within fibril SD(nm)	Within fibril CV(%)	Within fibril absolute slope(nm/μm)
Patellar	100 (35)	7.5 (3.3)	8.0 (4.0)	0.46 (0.35)
Semi-Automated (n = 100)	[64–226]	[1.1–21.7]	[1.5–26.9]	[0.00–1.45]
Hamstring	144 (66)	14.0 (4.9)	11.5 (6.3)	0.70 (0.51)
Semi-Automated (n = 100)	[60–387]	[2.8–27.8]	[2.0–30.1]	[0.00–2.20]
Patellar	123 (47)	8.7 (2.1)	7.6 (2.2)	0.58 (0.32)
Manual (n = 10)	[65–204]	[5.5–11.5]	[5.2–12.5]	[0.17–1.12]
Hamstring	155 (60)	10.1 (2.1)	7.0 (1.9)	0.28 (0.19)
Manual (n = 10)	[85–274]	[7.8–13.7]	[4.7–10.1]	[0.06–0.65]
Average across all	124 (57)	10.6 (5.1)	9.6 (5.4)	0.56 (0.44)
(n = 220)	[60–387]	[1.1–27.8]	[1.5–30.1]	[0.00–2.20]
Stapedius	52.8 (8.4)	–	–	–
Manual (n = 300)	[32.2–76.0]			

SD = standard deviation, CV = coefficient of variation, n = number of fibrils measured. Slope refers to the overall change in fibril diameter along the segmented length by linear regression. The absolute value is reported to remove direction dependence of the slope.

* Note that the absolute diameters do not represent the fibril diameter distribution in the tissue, only that of the fibrils used in the analysis of change along length.

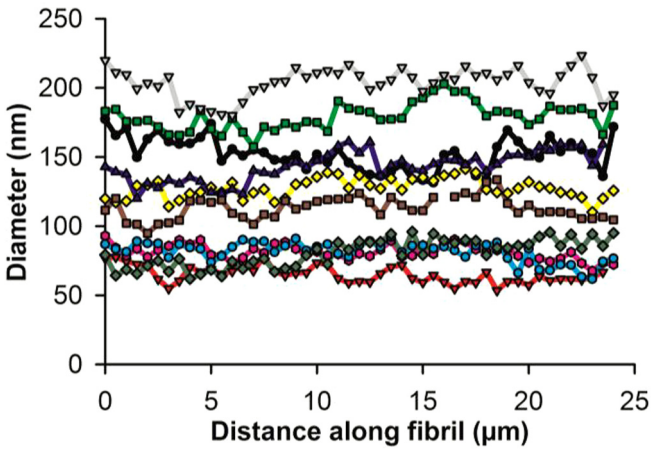

Fig. 6. Manually measured fibril diameters in the patellar tendon along the length of a FIB-SEM stack. Each line represents one fibril.

near a termination, most fibrils would not taper and then the maximum value of 2.20 nm/μm is more relevant. The semi-automated method also provide the coordinates of each fibril and from these we determined that the sections were around 5° off from perpendicular, which has an insignificant effect on the diameter measures (<0.5%). The fibrils in the stapedius tendon were thinner and more uniform in size than in the human tendons (Table 1).

4. Discussion

4.1. Fibril length

The original goal of this study was to trace individual collagen fibrils over macroscopic distances to unequivocally determine their length, but even with the current advanced serial imaging techniques we were unable to achieve this for a number of reasons. First, using the FIB-SEM method only a smaller region of the sample is milled away, and as the stack gets deeper the side walls cause artifacts. The microtome based method removes the entire surface but risks damaging the sample during sectioning because it needs to be long and thin. Furthermore, we initially expected to image each section in around 1 min leading to a 14 day acquisition time for a 2 mm long sample, but in order to achieve sufficient image quality each section on the mouse stapedius took around 4 min (~5 days for the 200 μm sample). In addition, deeper stacks would also require larger imaging areas because individual fibrils weave in and out of bundles causing them to "diffuse" across large parts of the sample cross-section, even when the sample itself remains well aligned. This means that if a field twice as large (60 μm) had to be imaged at sufficient quality, it would result in an acquisition time of ~200 days for a 2 mm long sample. Maintaining image quality for such a long run was deemed infeasible. Consequently we were relegated to a statistical approach similar to what has been done in the past [13], but with the more advanced techniques enabling us to cover a greater volume than previously. By virtue of the greater volume investigated, the present results push the estimate of fibril length even higher, from the several mm range to the tens of mm range, with an average exceeding the length of at least the patellar tendon (~50 mm). It should be kept in mind that the certainty of the fibril length is low, so within the 95% confidence limits, the fibrils could be down to 14 mm. Even at this limit, 14 mm would still be greater than what has previously been estimated, and while the fibrils would not be structurally continuous, they would almost certainly remain mechanically continuous as described later in the discussion. Another point of contention is the assumption that fibril ends are uniformly distributed, since we only examined a central portion of the human tendons. To our knowledge there is no evidence suggesting that ends would be localized in specific regions, and an uneven distribution of fibril ends would in general be detrimental to mechanical strength since regions with higher end-density would become weak points. Regardless of the average fibril length, the statistical approach cannot directly show if there are in fact continuous fibrils attached to muscle at one end and bone at the other. To help bridge this gap, a tendon (mouse stapedius), which is within the achievable dimensions for serial imaging (<200 μm long), was investigated. We managed to trace 5 fibrils through nearly the entire length of the stapedius tendon (missing the first few μm at the muscle insertion as previously mentioned) and did not observe any ends, proving that structurally continuous collagen fibrils exist in some tendons. In terms of function the stapedius tendon is not weight-bearing like patellar and hamstring tendons but morphologically it is similar (connecting muscle to bone) and it has a similar microstructure of dense collagen fibril bundles.

4.2. Tapering ends

It is generally expected that the ends of intact fibrils are tapered [23], and if they taper very slowly they would seem to slowly fade away rather than ending, which could cause difficulty in the observation of ends. For this to be a problem the taper would have to occur so slowly that the fibril would be near the detection limit of the imaging technique over the length of the segmented volume. In the present study most recordings had pixel resolutions of approximately 5 nm and a fibril would need to be at least several pixels in diameter to be reasonably traceable leading to a detection limit of around 30 nm. There is limited data on fibril taper, and to our knowledge none on mature fibrils, but a study on chick tendon at embryonic day 18 looked at the fibril taper shape and found that the number of molecules in a fibril cross-section changed at a constant rate along the taper, which occurred over roughly 1 μm (15 D-periods) in fibrils of 30–40 nm diameter [24]. The taper rate was reported to be 30 molecules per 67 nm D-period (450 molecules/μm) [24], and assuming that molecules of 1.5 nm diameter are densely packed in a fibril of 100 nm diameter (~4500 molecules in cross section), the total taper would stretch over 10 μm. However, the part where the fibril diameter is below 30 nm would be less than 1 μm because the constant taper rate in terms of molecules leads to a parabolic tip shape in terms of diameter. It is therefore highly unlikely that fibril ends were overlooked due to taper. In addition fibril diameter was fairly stable, at least over tens of micrometers (10.6 nm SD) in agreement with our previous observations using atomic force microscopy on individual fibrils [25], and the highest taper rate observed here (2.2 nm/μm) is far lower than expected near an end.

4.3. Lengthening mechanisms

Fibrils clearly grow in length during maturation, likely by tip-to-tip fusion of short fibril segments as seen in immature tissue [8,23], combined with accretion of collagen molecules onto existing fibrils, as seen during *in vitro* reconstitution of collagen [26]. In order for the fibrils to efficiently reinforce the matrix this process has to proceed at least until the fibrils reach the critical length; however, the same elongation process could continue and the natural end-point would be structurally continuous fibrils as suggested by the present finding. This seems like a reasonable process and would avoid the need for a mechanism to stop fibril elongation at some desirable length. However, it appears that such a mechanism does in fact exist. The molecules within a fibril are usually oriented in the same direction (unipolar), giving the fibril

a C- and an N-terminal end, and it has previously been reported that fibril segments can only fuse tip-to-tip through the C-tip of such a unipolar fibril [23]. Fibrils fusing between two C-terminal ends will generate N-N bipolar fibrils that cannot fuse to each other, thereby limiting longitudinal growth by fusion. The existence of such a growth limiting mechanism could be considered to support the notion of discontinuous fibrils. Further investigation will be required to address this issue but we suspect that controlled fibril elongation may primarily be important to enable sliding during tissue growth [27], after which fibrils eventually elongate to become continuous as indicated by the present results.

4.4. Other structural observations

While tracing the collagen fibrils a number of other structural features were also observed, which could be important for tendon function. Branched collagen fibrils have been reported in the past [28,29] and were also observed here, although the prevalence in the present study (1:250,000 D-periods) was lower than previously reported for embryonic mouse tails (1:20,000 D-periods) [28]. Whether such a branch represents fibril splitting, fusion or perhaps a nucleation site of fibril growth is not known. The "merged" fibril region could in principle be two closely associated but still individual fibrils; however, in 3 of the 4 observed branches the fibrils were of equal size and thus the merged region should have been elliptical if they simply coursed alongside each other, which was not the case. In all 4 cases the merged region had greater diameter than either of the two branches, but only in one case was the merged cross-sectional area equal to the sum of the branches, in the remaining three the area was between 60% and 80% of the sum. If branches occur randomly then the observation that fibrils branch more often than they terminate would indicate that they on average have a branch point connecting them to a neighboring fibril before terminating. As previously suggested this would lead to a structurally connected branched network of collagen fibrils [29]. However, the observation that all of the fibril branches were found within a relatively small region could indicate that they do not occur randomly. An alternative possibility is that fibril fusion may be a mechanism for repairing local fibril damage. The hypothesis would be that the ends of a broken fibril fuse onto the shafts of nearby intact fibrils to maintain continuity. The mechanical damage itself could facilitate this mechanism by disrupting the proteoglycans that would normally keep the fibrils from fusing [8,23]. Such a mechanism would enable a form of self-healing that is independent on cellular activity and turnover. We have no overt evidence for such a mechanism, but it could be worth investigating in the future. A previous study, which may lend some support to the idea, reported that fibrils in the scar region of healing ligaments are continuous with fibrils in the intact tissue, and that qualitatively there appeared to be an increased occurrence of fibril branches in the interface region [30].

In several cases fibrils were seen to bend back on themselves in a hairpin loop, sometimes continuing all the way back through the stack and sometimes going back for several μm before making another turn and continuing through the stack in the original direction again. The fibrils in question were not particularly thin (average diameter 93 nm) or otherwise remarkable, indicating that it is probably not just a subpopulation of "loose" fibrils. The presence of such loops suggests that fibrils are not taut within the matrix, but their origin is not clear. We suspect that fibrils of varying lengths exist within a tendon (even if they are continuous) and that these are sequentially recruited during mechanical stretching. In that case the longest fibrils would have to be bent or buckled in the unloaded tendon, which could give rise to the observed loops on the fibril. The difference in fibril length could be generated by simply forming non-straight fibrils, but could also occur by formation of straight fibrils in the stretched state of the tendon.

4.5. Continuous vs. discontinuous fibrils

In composite materials science a key concept is the "critical length", defined as the length at which the surface area of a fiber is large enough that the bonding strength to its surroundings matrix becomes greater than the strength of the fiber itself. A fiber longer than its critical length will break rather than slipping. Little is known about the mechanisms and magnitude of interfibrillar shear load transmission in tendons. A recent study used a notch testing method to estimate an interfibrillar shear strength of 32 kPa under quasi static conditions [16]. The strength of collagen fibrils is also poorly investigated, but we have previously determined a value of 540 MPa for hydrated human patellar tendon fibrils normalized to their dry cross-sectional area [31]. For a native tendon the hydrated cross-section should be used and assuming a 30% increase in diameter upon hydration [32] the native fibril strength becomes 320 MPa. With the average diameter in the present study of 125 nm, the critical length can be estimated to be 625 μm. The numbers used in this calculation are somewhat uncertain but it seems fair to assume that the majority of fibrils will have critical lengths around 1 mm. Other studies investigating fibril length in mature tissue have found values in the range 0.86–12.7 mm, indicating that most fibrils may exceed their critical length [13–15]. This is in agreement with the observation that only broken fibrils can be isolated from mature tendon tissues [8].

Combining these considerations with the present findings, it appears that in mature tendon many of the fibrils are structurally continuous. In addition they are also mechanically continuous independent of their structural continuity, because their lengths exceed the critical length. Furthermore, even given their structural continuity the fibrils are not necessarily taut but may be sequentially recruited. To the extent that fibrils exceed the critical length, failure will occur by fibril breakage, whether they are continuous or not, and when the fibrils are broken continuity is lost and there is no distinction between continuous and discontinuous cases. That fibrils are loaded to their mechanical limit rather than slipping during tendon failure is supported by recent *in vitro* studies showing that tendons overloaded into the region of plastic deformation display fibril damage at discrete locations, which increases in frequency with repeated overloading [33]. Similar localized damage was reported years ago in conjunction with X-ray diffraction, showing that intrafibrillar damage mechanisms – that did not alter the average fibril D-period (strain) – preceded interfibrillar sliding and macroscopic failure [34].

A major contention against structural continuity of fibrils, is the observation that tendons [35] and ligaments [36] can creep to failure even under relatively low loads, and furthermore X-ray diffraction has shown that while the tendon elongates during creep, the fibril D-period (fibril strain) remains constant [17]. Such behavior can be explained by fibril slippage, but if fibrils are continuous they should eventually become taut and resist further deformation before failing. Individual fibrils also display viscous behavior and can be expected to creep themselves, which could explain the macroscopic creep even after fibrils are taut [37]. However, such intra-fibrillar creep would lead to molecular sliding and likely increase the D-period, which is not consistent with the X-ray observations. It is worth noting that while the D-period did not increase in the X-ray study, other changes in the diffraction pattern were observed [17], indicating that some structural changes took place within the fibril during creep. If these changes were related to localized fibril damage as mentioned previously, it is possible that individual fibrils break sequentially during the creep process,

thereby leading to a discontinuous structure that can creep further by interfibrillar sliding.

5. Conclusion

Collagen fibril ends within mature human tendon are extremely rare, in agreement with previous reports. The significant fibril volume investigated in the present study provides statistical evidence that fibrils may even be structurally continuous. This finding is supported by our results on the short mouse stapedius tendon in which fibril continuity could be directly observed. In some aspects, tendon behaves mechanically as a material with discontinuous fibrils; however, this observation could possibly be explained if localized damage causes collagen fibrils to sequentially break, thereby leading to an effectively discontinuous fibril network as damage accumulates. Our findings support fibril breakage rather than slippage as the primary mode of tissue damage and consequently maintenance and repair mechanisms should be expected to deal with regenerating broken fibrils.

Funding

This work was supported by the Danish Council for Independent Research: Medical Sciences (DFF – 1333-00052A). The funding bodies had no influence on the study.

Disclosures

All authors declare no conflicting interests.

Contributions

Conception and design: RBS, KQ, SPM. Laboratory work: RBS, AH, TS, ML, KQ. Data analysis: RBS, TS. Interpretation and discussion: RBS, AH, TS, ML, KK, KQ, SPM. Review and approval of manuscript: RBS, AH, TS, ML, KK, KQ, SPM.

Acknowledgements

We thank the orthopedic surgeons at Bispebjerg Hospital for collecting human tissue specimens and Peter Schjerling for invaluable discussion and ideas.

Appendix A. Supplementary data

Supplementary data associated with this article can be found, in the online version, at http://dx.doi.org/10.1016/j.actbio.2017.01.006.

References

[1] E.H. Epstein, [α1(III)]$_3$ human skin collagen – release by pepsin digestion and preponderance in fetal life, J. Biol. Chem. 249 (1974) 3225–3231.
[2] K. Gelse, E. Poschl, T. Aigner, Collagens – structure, function, and biosynthesis, Adv. Drug Deliv. Rev. 55 (2003) 1531–1546.
[3] M. van der Rest, R. Garrone, Collagen family of proteins, FASEB J. 5 (1991) 2814–2823.
[4] J.Y. Exposito, U. Valcourt, C. Cluzel, C. Lethias, The fibrillar collagen family, Int. J. Mol. Sci. 11 (2010) 407–426.
[5] K.M. Heinemeier, P. Schjerling, J. Heinemeier, S.P. Magnusson, M. Kjaer, Lack of tissue renewal in human adult achilles tendon is revealed by nuclear bomb (14)c, FASEB J. 27 (2013) 2074–2079.
[6] J.P. Gumucio, A.C. Phan, D.G. Ruehlmann, A.C. Noah, C.L. Mendias, Synergist ablation induces rapid tendon growth through the synthesis of a neotendon matrix, J. Appl. Physiol. 117 (2014) 1287–1291.
[7] D.A.D. Parry, A.S. Craig, Collagen fibrils and elastic fibers in rat-tail tendon: An electron microscopic investigation, Biopolymers 17 (1978) 843–845.
[8] D.E. Birk, M.V. Nurminskaya, E.I. Zycband, Collagen fibrillogenesis in situ: Fibril segments undergo post-depositional modifications resulting in linear and lateral growth during matrix development, Dev. Dyn. 202 (1995) 229–243.
[9] D.E. Birk, E.I. Zycband, D.A. Winkelmann, R.L. Trelstad, Collagen fibrillogenesis in situ: Fibril segments are intermediates in matrix assembly, Proc. Natl. Acad. Sci. USA 86 (1989) 4549–4553.
[10] M.S. Hansen, M. Christensen, T. Budolfsen, T.F. Ostergaard, T. Kallemose, A. Troelsen, K.W. Barfod, Achilles tendon total rupture score at 3 months can predict patients' ability to return to sport 1 year after injury, Knee Surg. Sports Traumatol. Arthrosc. 24 (2016) 1365–1371.
[11] P. Eliasson, C. Couppe, M. Lonsdale, R.B. Svensson, C. Neergaard, M. Kjaer, L. Friberg, S.P. Magnusson, Ruptured human achilles tendon has elevated metabolic activity up to 1 year after repair, Eur. J. Nucl. Med. Mol. Imaging (2016), http://dx.doi.org/10.1007/s00259-016-3379-4.
[12] I.Z. Nagy, H.P. von Hahn, F. Verzar, Age-related alterations in the cell nuclei and the DNA content of rat tail tendon, Gerontologia 15 (1969) 258–264.
[13] P.P. Provenzano, R. Vanderby, Collagen fibril morphology and organization: Implications for force transmission in ligament and tendon, Matrix Biol. 25 (2006) 71–84.
[14] A.S. Craig, M.J. Birtles, J.F. Conway, D.A.D. Parry, An estimate of the mean length of collagen fibrils in rat tail-tendon as a function of age, Connect. Tissue Res. 19 (1989) 51–62.
[15] F.H. Silver, D.L. Christiansen, P.B. Snowhill, Y. Chen, Role of storage on changes in the mechanical properties of tendon and self-assembled collagen fibers, Connect. Tissue Res. 41 (2000) 155–164.
[16] S.E. Szczesny, J.L. Caplan, P. Pedersen, D.M. Elliott, Quantification of interfibrillar shear stress in aligned soft collagenous tissues via notch tension testing, Sci. Rep. 5 (2015) 14649.
[17] W. Folkhard, W. Geercken, E. Knorzer, E. Mosler, H. Nemetschekgansler, T. Nemetschek, M.H.J. Koch, Structural dynamic of native tendon collagen, J. Mol. Biol. 193 (1987) 405–407.
[18] A. Herchenhan, M.L. Bayer, R.B. Svensson, S.P. Magnusson, M. Kjaer, In vitro tendon tissue development from human fibroblasts demonstrates collagen fibril diameter growth associated with a rise in mechanical strength, Dev. Dyn. 242 (2013) 2–8.
[19] T. Starborg, N.S. Kalson, Y. Lu, A. Mironov, T.F. Cootes, D.F. Holmes, K.E. Kadler, Using transmission electron microscopy and 3view to determine collagen fibril size and three-dimensional organization, Nat. Protoc. 8 (2013) 1433–1448.
[20] A.J. Bushby, K.M.Y. P'ng, R.D. Young, C. Pinali, C. Knupp, A.J. Quantock, Imaging three-dimensional tissue architectures by focused ion beam scanning electron microscopy, Nat. Protoc. 6 (2011) 845–858.
[21] J.R. Kremer, D.N. Mastronarde, J.R. McIntosh, Computer visualization of three-dimensional image data using imod, J. Struct. Biol. 116 (1996) 71–76.
[22] C.A. Schneider, W.S. Rasband, K.W. Eliceiri, Nih image to imagej: 25 years of image analysis, Nat. Methods 9 (2012) 671–675.
[23] H.K. Graham, D.F. Holmes, R.B. Watson, K.E. Kadler, Identification of collagen fibril fusion during vertebrate tendon morphogenesis. The process relies on unipolar fibrils and is regulated by collagen-proteoglycan interaction, J. Mol. Biol. 295 (2000) 891–902.
[24] D.F. Holmes, H.K. Graham, K.E. Kadler, Collagen fibrils forming in developing tendon show an early and abrupt limitation in diameter at the growing tips, J. Mol. Biol. 283 (1998) 1049–1058.
[25] R.B. Svensson, T. Hassenkam, C.A. Grant, S.P. Magnusson, Tensile properties of human collagen fibrils and fascicles are insensitive to environmental salts, Biophys. J. 99 (2010) 4020–4027.
[26] D.A. Cisneros, C. Hung, C.A. Franz, D.J. Muller, Observing growth steps of collagen self-assembly by time-lapse high-resolution atomic force microscopy, J. Struct. Biol. 154 (2006) 232–245.
[27] M.L. Wood, G.E. Lester, L.E. Dahners, Collagen fiber sliding during ligament growth and contracture, J. Orthop. Res. 16 (1998) 438–440.
[28] T. Starborg, Y. Lu, A. Huffman, D.F. Holmes, K.E. Kadler, Electron microscope 3d reconstruction of branched collagen fibrils in vivo, Scand. J. Med. Sci. Sports 19 (2009) 547–552.
[29] K.E. Kadler, D.F. Holmes, H. Graham, T. Starborg, Tip-mediated fusion involving unipolar collagen fibrils accounts for rapid fibril elongation, the occurrence of fibrillar branched networks in skin and the paucity of collagen fibril ends in vertebrates, Matrix Biol. 19 (2000) 359–365.
[30] P.P. Provenzano, C. Hurschler, R. Vanderby Jr., Microstructural morphology in the transition region between scar and intact residual segments of a healing rat medial collateral ligament, Connect. Tissue Res. 42 (2001) 123–133.
[31] R.B. Svensson, H. Mulder, V. Kovanen, S.P. Magnusson, Fracture mechanics of collagen fibrils: Influence of natural cross-links, Biophys. J. 104 (2013) 2476–2484.
[32] K.M. Meek, N.J. Fullwood, P.H. Cooke, G.F. Elliott, D.M. Maurice, A.J. Quantock, R.S. Wall, C.R. Worthington, Synchrotron x-ray diffraction studies of the cornea, with implications for stromal hydration, Biophys. J. 60 (1991) 467–474.
[33] S.P. Veres, J.M. Harrison, J.M. Lee, Repeated subrupture overload causes progression of nanoscaled discrete plasticity damage in tendon collagen fibrils, J. Orthop. Res. 31 (2013) 731–737.
[34] E. Knorzer, W. Folkhard, W. Geercken, C. Boschert, M.H. Koch, B. Hilbert, H. Krahl, E. Mosler, H. Nemetschek-Gansler, T. Nemetschek, New aspects of the etiology of tendon rupture. An analysis of time-resolved dynamic-mechanical measurements using synchrotron radiation, Arch. Orthop. Trauma. Surg. 105 (1986) 113–120.

[35] X.T. Wang, R.F. Ker, Creep rupture of wallaby tail tendons, J. Exp. Biol. 198 (1995) 831–845.
[36] G.M. Thornton, T.D. Schwab, T.R. Oxland, Cyclic loading causes faster rupture and strain rate than static loading in medial collateral ligament at high stress, Clin. Biomech. 22 (2007) 932–940.
[37] R.B. Svensson, T. Hassenkam, P. Hansen, S.P. Magnusson, Viscoelastic behavior of discrete human collagen fibrils, J. Mech. Behav. Biomed. Mater. 3 (2010) 112–115.